Periodic orbit quantization of bound chaotic systems

1991 J. Phys. A: Math. Gen. 24 4763

(http://iopscience.iop.org/0305-4470/24/20/012)

J. Phys. A: Math. Gen. 24 (1991) 4763-4778. Printed in the UK

Periodic orbit quantization of bound chaotic systems

Per Dahlqvist† and Gunnar Russberg‡

† Nordisk Institut for Teoretisk Fysik, Blegdamsvej 17, DK-2100 Copenhagen Ø, Denmark
‡ Fachbereich Physik der Philipps-Universität, Renthof 6, 3550 Marburg, Federal Republic of Germany

Received 22 April 1991, in final form 10 June 1991

Abstract. We present periodic orbit quantizations of the hyperbola billiard and the x^2y^2 potential. These two systems may be considered as belonging to the one-parameter family of potentials $(x^2y^2)^{1/a}$. The quantum states are determined by means of the zeros of an expanded and truncated Selberg zeta function. The symmetries of the problem are considered and the Selberg zeta function is factorized into the irreducible representations of the symmetry group. The thus calculated eigenenergies are in good agreement with quantum mechanical calculations and converge when the number of terms in the expansion is increased. The results strongly indicate that the trace formula provides individual quantum eigenstates for chaotic systems.

1. Introduction

The correspondence principle tells us that a quantum theory, in order to be consistent, must yield the laws of classical mechanics in the limit $\hbar \to 0$. How this transition is realized in practice has been the objective of extensive research. When studying the relations between the quantum and classical behaviour of Hamiltonian systems with few degrees of freedom, semiclassical methods like Einstein–Brillouin–Keller (EBK) quantization have proven remarkably useful. However, EBK quantization relies on the presence of invariant tori, i.e. it is only applicable on integrable and near-integrable systems. There has been an extensive search for a corresponding scheme for ergodic and mixed systems. The trace formula by Gutzwiller [1, 2] seems to offer a possible way to go. This formula relates the density of eigenenergies to dynamical invariants of the periodic orbits of a system:

$$g(E) = g_0(E) + \frac{1}{i\hbar} \sum_p T_p \sum_{n=1}^{\infty} \frac{1}{|A_p^n - I|^{1/2}} \exp\left[in\left(S_p/\hbar - \mu_p \frac{\pi}{2} \right) \right]. \tag{1}$$

Here $g(E) = \mathrm{Tr}\, G(q, q'; E)$ is the trace of the semiclassical Green function, and the density of eigenstates is simply given by $d(E) = -(1/\pi) \lim_{\varepsilon \to 0} \mathrm{Im}\, g(E + i\varepsilon)$. The index p labels the primitive periodic orbits, S_p is the action integral along the orbit, T_p $(= \partial S_p / \partial E)$ its period, and A_p is the linearized Poincaré map around the orbit. The phase index μ_p is commonly referred to as the Maslov index. Finally, $g_0(E)$ provides the mean level distribution, which may be interpreted as the contribution from classical orbits of zero length.

Applied to an integrable system the trace formula provides quantization conditions similar to those of EBK [3, 4]. If, on the other hand, the system is ergodic, i.e. all

0305-4470/91/204763+16$03.50

periodic orbits are unstable, the quantum eigenstates seem to be built up through a complicated inteference of many periodic orbits. In spite of its simple appearance, direct use of the trace formula to evaluate quantal spectra of chaotic systems has not been practiced except in a few cases [5-9]. There are two main reasons for this:

(i) the periodic orbit structure of a chaotic system is usually more complicated and difficult to determine than the exact quantum eigenenergies:

(ii) due to the exponential proliferation of long periodic orbits the sum (1) is at best conditionally convergent.

Difficulty (i) may be reduced if one can find a good *symbolic dynamics* for the system, i.e. a scheme that assigns a unique symbol string (coding) to each periodic orbit. Through difficulty (ii) there is a certain need for refined summation techniques; these will benefit from the firm control of the periodic orbit structure that is given by a good symbolic dynamics.

Symbolic dynamics has so far been developed for some simple scattering systems [10, 11], the anisotropic Kepler problem [8] and the quadratic Zeeman effect [12]. Refined summation techniques using zeta functions have been applied to open three- and four-disc scattering systems with good results [10, 11]. The introduction of zeta functions is motivated by the observation that the second term in (1) can be written as the logarithmic derivative of a Selberg zeta function, i.e.

$$g(E)-g_0(E)=\frac{\mathrm{d}}{\mathrm{d}E}\ln Z(E) \tag{2}$$

where $Z(E)$ is defined as the infinite product

$$Z(E)=\prod_{p}\prod_{k=0}^{\infty}(1-t_p\Lambda_p^{-k}). \tag{3}$$

The quantum weights t_p in (3) are given by

$$t_p=\frac{\exp[\mathrm{i}(S_p/\hbar-\mu_p\pi/2)]}{|\Lambda_p|^{1/2}}. \tag{4}$$

Attention has here been restricted to systems with two degrees of freedom: the eigenvalues of A_p are Λ_p, Λ_p^{-1}, where $\Lambda_p=\pm\exp u$ or $\Lambda_p=\exp \mathrm{i}u$, and $u\geqslant 0$ is real [14]. Equation (4) is valid for unstable orbits (real eigenvalues); the inclusion of stable orbits (complex eigenvalues) requires slight modifications of (1) and (4) [2]. For a generic Hamiltonian relation (2) is true only to leading order in $\hbar$, but for homogenous Hamiltonians, like those considered in this paper, it is actually exact.

The purpose of the present paper is to apply a refined summation technique to some *bound* Hamiltonian systems. We will study the Hamiltonian

$$H=\tfrac{1}{2}(p_x^2+p_y^2+x^2y^2) \tag{5}$$

appearing in the long wavelength limit of SU(2) Yang-Mills theories [15]. A similar system describes a hydrogen atom in a very strong magnetic field (the quadratic Zeeman effect) [12]. The system (5) has for a long time been believed to exhibit ergodic motion, but as we showed in [16] there exists at least one family of stable periodic orbits. Nevertheless, an overwhelming portion of phase space is occupied by chaotic motion, so it is still a suitable system for our purposes.

We will also study the hyperbola billiard, i.e. a particle moving freely inside four hard reflecting walls determined by the equality

$$|xy| = 1. \tag{6}$$

Due to the concavity of the walls, all periodic orbits in this system are unstable [9]. A little modified, the system (6) (and (5) as well) may be used to model certain mesoscopic systems [17].

The systems (6) and (5) belong to the one-parameter family of Hamiltonians,

$$H = \tfrac{1}{2}[p_x^2 + p_y^2 + (x^2y^2)^{1/a}] \tag{7}$$

where the quartic potential (5) is obtained for $a = 1$ and the hyperbola billiard (6) is obtained in the limit $a \to 0$.

In section 2 we present a symbolic coding for the systems (7). We also show how stable orbits may occur when $a > 0$. In section 3 we briefly review how the Selberg product factorizes into the irreducible representations of the symmetry group of the particular problem. We then expand this product and define a sequence of approximants to the infinite Selberg product. In section 4 we show how the zeros of this approximate Selberg product converge, thus giving us the quantum eigenenergies. We also briefly discuss the numerical techniques used to find the period orbits and their invariants. We round off with a discussion in section 5.

2. Symbolic dynamics

The systems (7) are invariant under the group C_{4v}. Considering the four branches of the hyperbolas in (6) as discs we can label (periodic) orbits of the hyperbola billiard similarly to those of a symmetric four-disc system [9, 12, 13].

We use a three-character alphabet $A = \{2, 1, 0\}$ to label the orbits: The scattering events (bounces) in a four-disc billiard are well defined in phase space, and each single scattering event is associated with a letter from the alphabet. Scattering from one disc to the diagonally opposite disc is given the code 2. Scattering to a neighbouring disc is given to the code 1 if the last scattering to a nearest neighbour (thus not counting any cross-diagonal scatterings in between) was equally directed (clockwise or anticlockwise), and 0 if oppositely directed.

Any closed orbit in the four-disc system defines a periodic bi-infinite sequence of symbols. A *primitive*, or prime, periodic orbit is the shortest non-repeating traversal of a closed orbit. A primitive symbol sequence is analogously the shortest non-repetitive part of a periodic sequence. We let a point at the beginning and at the end of a symbol string denote that it is periodic, thus .210. means... 102102102102102102.... All cyclic permutations of a given primitive sequence are regarded as identical.

Primitive sequences built up by the rules above correspond to families of distinct periodic orbits. The members of a certain family (all associated with the same symbol code) are related to each other via the transformations of the symmetry group, and they are all mapped onto the same single orbit in the *fundamental domain*. The fundamental domain is the region restricted by the symmetry lines $y = 0$ and $y = x$, which are treated as hard walls; it is the smallest non-symmetric region on which all orbits of the full system may be mapped. In the fundamental domain the labelling as defined above is unique, i.e. there cannot be two periodic orbits associated with the

same primitive symbol sequence. A periodic orbit in the full domain may correspond to more than one traversal of the prime symbol sequence (and thus of the periodic orbit in the fundamental domain). In these cases the orbit in the full domain consists of several (two or four in the C_{4v} case) equivalent pieces.

In a system of well-separated discs all symbol sequences are realized as orbits in the system. However, in the hyperbola billiard some orbits are for geometrical reasons excluded, one speaks of *pruning* of the symbol dynamics. Two such examples are the sequences $.210^{k}.$ and $.10^{k+2}.$, which are pruned for $k>3$.

By means of (7) we can define a one-to-one correspondence between orbits in the hyperbola billiard and orbits in the x^2y^2 potential. Since the bounces are no longer well defined for $a>0$, we cannot use the bounce events to define a Poincaré surface of section, instead we choose as surface of section the wall $y=0$ in the fundamental domain. If n_2 is the number of 2s, n_1 the number of 1s and n_0 the number of 0s in a symbol string p, the corresponding orbit will intersect the surface of section $n=2n_2+n_1+n_0$ number of times. The reason is that a diagonal scattering (associated with the symbol 2) crosses both the $y=0$ and $x=0$ lines. Both these symmetry lines are mapped onto $y=0$ in the fundamental domain and thus a diagonal scattering corresponds to two crossings of the surface of section. Continuity requires that a scattering through the origin is regarded as having two intersections. A scattering to a nearest neighbour (associated with symbol 1 or 0) crosses either $y=0$ or $x=0$, i.e. there is only one crossing of the surface of section in the fundamental domain.

Figure 1 provides a selection of periodic orbits in the x^2y^2 potential, presented both in the full and the fundamental domain.

Not all orbits present in the hyperbola billiard exist in the x^2y^2 potential. When a is increase some of them will be (dynamically) pruned through inverse bifurcations. This happens to, for example, .210. and .1000.. We note that these two orbits have the same topology and make the same number of crossings ($n=4$) with the surface of section. As a increases and the potential softens, the orbits approach each other (see figure 2.) until, at $a\approx 0.62$, they coincide and disappear via a tangent bifurcation. In figure 3 we have plotted the trace of the monodromy matrix, $\mathrm{Tr}(M)$, for all orbits with $n=4$, 8, 12 and 16 participating in the associated bifurcation cascade. We see that in this parameter region some orbits are occasionally stable ($-2<\mathrm{Tr}(M)<2$) and global ergodicity is thus destroyed over a finite interval in the parameter a. If we define a new two-character alphabet, $B=\{210, 0100\}$, one may conjecture that all primitive periodic sequences built from this alphabet are being pruned during the bifurcation cascade. At still lower values of the parameter a, the pairs of orbits .2100. and .10000., and .21000. and .100000., respectively, have undergone similar pruning cascades; at $a=1$ one pruning rule will be $.210^{k}.$ and $.10^{k+2}.$ are pruned for $k>0$ (to be compared with the case $a=0$ above; $k>3$).

A further pruning cascade occurs in the vicinity of $a=1.0$ (see figure 4). This one is more complicated since there are two 2s in the symbol sequence. $220^{7}.$; each 2 is associated with an uncertainty whether to go the the diagonal 'disc' directly or via a 'bounce' onto a nearest neighbour 'disc'. This consideration gives $.2110^{7}.$, $.01210^{6}.$ and $.01010^{7}.$ as close relatives that will also be pruned in the cascade. The orbits $.220^{7}.$ and $.01010^{7}.$ are singlets under time reversal and $.2110^{7}.$ and $.01210^{6}.$ is a doublet. Singlets are recognized as librations in the fundamental domain and doublets as rotations. (see figure 1; the four orbits in figures 1(d–f) only differ from these four by two 0s in the symbol code. Thus they are further away from bifurcation and easier to distinguish visually.) Note that the doublet above is stable when $a=1$ (the existence of this

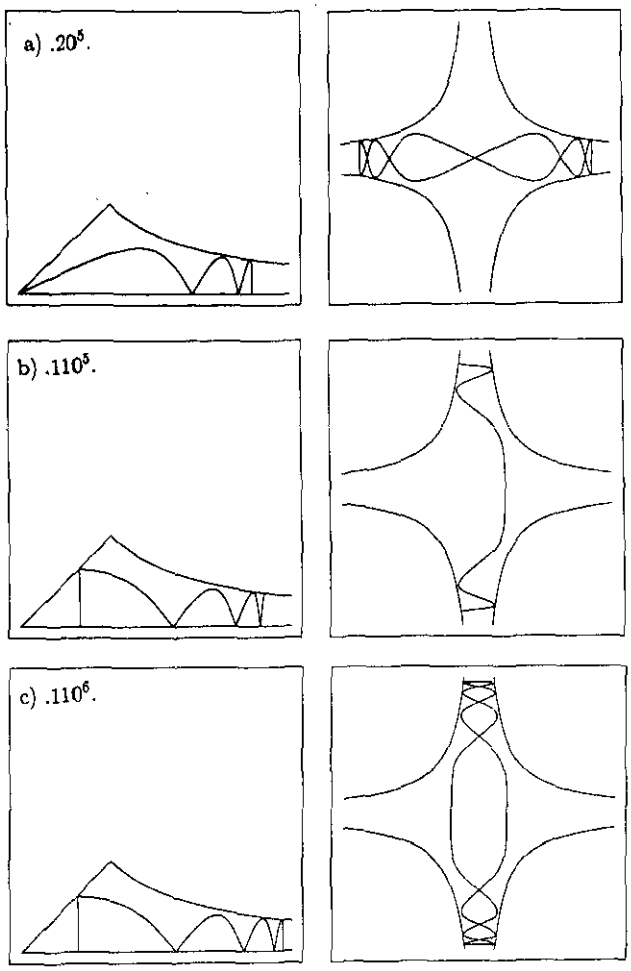

Figure 1. A selection of periodic orbits in the x^2y^2 model. The contour $x^2y^2 = 1$ encloses the energetically allowed region.

'ergodicity-destroying' orbit has been reported elsehwere [16]). The complexity of this pruning cascade is well illustrated by the fate of the orbit $.220^7\ 01010^7$. (see figure 3). First it absorbs the doublet ($.220^7\ 2110^7$., $.220^7\ 01210^6$.) in a bifurcation at $a \approx 1.024$. Then it makes a dip far below the plot and it is eventually killed by $.220^7$. through a pitch fork bifurcation at $a \approx 1.067$.

We note that figures 3 and 4 indicate that the symbol codes are unique even in connection with these cascades and the result strongly suggests that the pruning process is monotonous in the sense that orbits are killed but never born when the parameter a is increased.

A dominating feature of the systems (7) is the intermittent oscillations in the potential 'arms'. These oscillations correspond to orbits that contain long substrings of 0s in the symbol code. There are sequences of allowed (periodic) strings $.p_0 0^k.$, like the $.20^k.$ and $.110^k.$ families, which have no limit in the number of 0s. As we have already seen examples of, there also exist sequences that are pruned after a certain number of 0s.

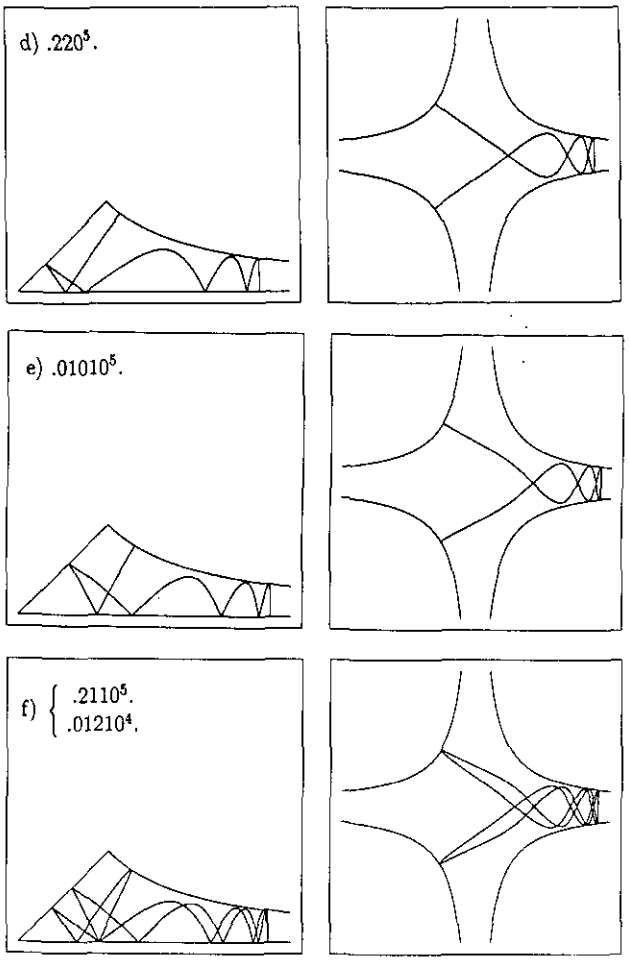

Figure 1. (continued)

3. Symmetry-projected zeta functions

In [8, 10, 18, 20] discrete symmetries are taken into account in connection with the periodic orbit theory, and in [5, 19] the correct description was given for orbits running along symmetry lines, orbits we will refer to as *boundary orbits.*

The zeta function $Z(E)$ in (3) is written as a product $\Pi_r Z_r(E)$ over r, the irreducible representations of the group, and each Z_r is given by

$$Z_r(E) = \prod_{\bar{p}} \prod_{k=0}^{\infty} (1 - t_{\bar{p}} \Lambda_{\bar{p}}^{-k}) \tag{8}$$

where the weights $t_{\bar{p}}$ for the one-dimensional representations are given by

$$t_{\bar{p}} = \chi_r(g_{\bar{p}}) \frac{\exp[i(S_{\bar{p}}/\hbar - \mu_{\bar{p}}\pi/2)]}{|\Lambda_{\bar{p}}|^{1/2}}. \tag{9}$$

All quantities now refer to periodic orbits in the fundamental domain, $\bar{p}$, indicated by the overbar. $\chi_r(g_{\bar{p}})$ is the group character of the representation r and $g_{\bar{p}}$ is the group

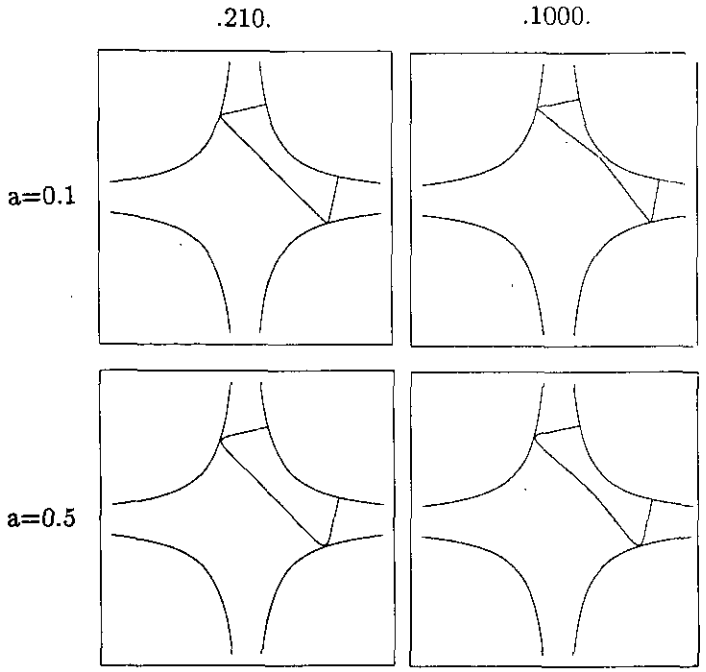

Figure 2. The orbits .210. and .0100. in the potential $V=\frac{1}{2}(x^2y^2)^{1/a}$ for different values of the parameter a.

element obtained as the product of group factors associated with the reflections of the domain walls (see next section). The index $\bar{p}$ runs through all primitive periodic orbits in the fundamental domain; thanks to the compact definition of the symbolic coding, this means it runs over all non-pruned prime symbol sequences. The zeros of the zeta function Z_r now correspond to quantum states with symmetries given by representation r. We continue by expanding the inner product in (8) according to Euler's identity:

$$Z(E)=\prod_{\bar{p}}\sum_{m=0}^{\infty}\frac{\Lambda_{\bar{p}}^{-m(m-1)/2}}{\prod_{i=1}^{m}(1-\Lambda_{\bar{p}}^{-i})}t_{\bar{p}}^{m} \tag{10}$$

$$=\prod_{\bar{p}}\sum_{m=0}^{\infty}C_{\bar{p},m}\exp\left[\mathrm{i}\left(mS_{\bar{p}}/\hbar-m\mu_{\bar{p}}\frac{\pi}{2}\right)\right]. \tag{11}$$

If we now expand the outer product, the zeta function can be written as a sum over all distinct sets $n=[m_{\bar{p}}]$, (called pseudo-orbits in [21]):

$$Z(E)=\sum_{n}C_n\exp\left[\mathrm{i}\left(S_n-\mu_n\frac{\pi}{2}\right)\right] \tag{12}$$

where we have defined the quantities

$$C_n=\prod_{\bar{p}}C_{\bar{p},m_{\bar{p}}} \tag{13}$$

$$S_n=\sum_{\bar{p}}m_{\bar{p}}S_{\bar{p}} \tag{14}$$

$$\mu_n=\sum_{\bar{p}}m_{\bar{p}}\mu_{\bar{p}}. \tag{15}$$

One can, at best, hope for conditional convergence of this sum, and one therefore has

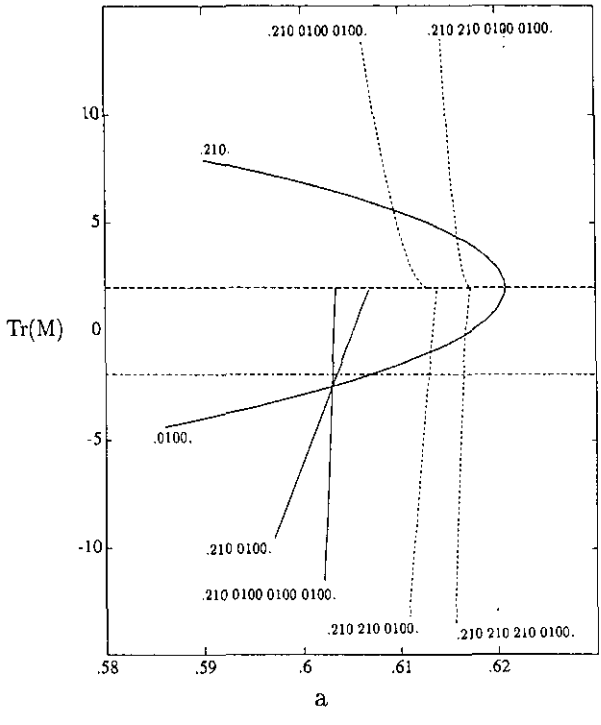

Figure 3. The trace of the monodromy matrix, $\mathrm{Tr}(M)$, as a function of a, for some selected orbits participating in the bifurcation associated with the pruning of the orbits in figure 2. The full curves are associated with tangent and pitchfork bifurcations and the broken ones with higher-order bifurcations.

to be careful when ordering the terms. A natural choice is to order the terms in (12) by decreasing order in $|C_n|$. We define

$$Z_N(E) = \sum_{n \leq N} C_n \exp\left[i\left(S_n - \mu_n \frac{\pi}{2} \right) \right] \tag{16}$$

where we let n also denote the position in the sequence of the corresponding set. The crucial question is now whether the zeros of $Z_N(E)$ approximate the zeros of $Z(E)$, and whether they converge when $N \to \infty$.

As was mentioned before, the boundary orbit must be given a special treatment. The result of such an analysis is that for the representations A_1 and B_2 the product in (8) is to include only *even* values of k, and for the representations A_2 and B_1 only *odd* values. The amplitudes C_n have to be modified accordingly.

4. Computation and results

Periodic orbits of the hyperbola billiard are obtained from an extremum principle in accordance with [9]. The stability eigenvalues are also obtained according to [9]. Periodic orbits in the system (5) are then found by adiabatically increasing the parameter a in (7) and tracing the fixed points on the Poincaré surface of section $y = 0$ with a Newton method. The equations of motion are solved using a fourth-order Runge–Kutta method, and the stability eigenvalues are now obtained by solving the linearized

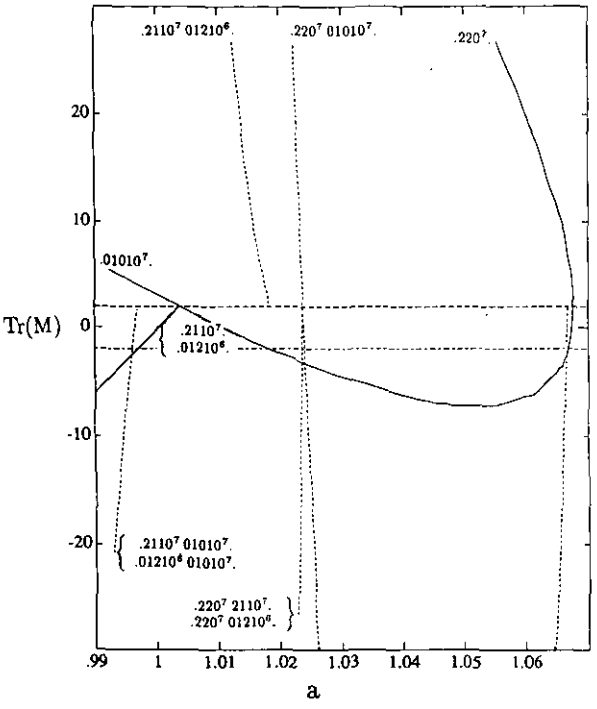

Figure 4. The trace of the monodromy matrix for some orbits participating in a pruning cascade in the vicinity of $a = 1$. The brackets embrace orbits related by time translation symmetry.

equations of motion around the particular orbit. Care has to be taken with the signs of the eigenvalues, since the dynamics is defined inside the fundamental domain. One finds that $\operatorname{sgn}(\Lambda_p) = (-1)^{n_2+n_1}$.

The group characters $\chi_r(g_p)$ are also conveniently expressed in terms of n_2, n_1 and n_0:

$$\chi_r(g_p) = \begin{cases} 1 \\ (-1)^{n_0} \\ (-1)^{n_1} \\ (-1)^{n_1+n_0} \end{cases} \qquad r = \begin{cases} A_1 \\ A_2 \\ B_1 \\ B_2. \end{cases} \tag{17}$$

A simple intuitive interpretation of these rather abstract factors would be to regard them as 'additional phase indices'. The quantum states of a certain representation (say B_1) are the same as those of a quantum system defined on the fundamental domain with certain boundary conditions imposed on the domain walls. In the B_1 case, for instance, we have Neumann boundary conditions on the line $y = 0$ and Dirichlet boundary conditions on the line $y = x$. An orbit bouncing on a 'Dirichlet wall' aquires a phaseshift π whereas a bounce on a 'Neumann wall" aquires zero phaseshift, according to familiar wave dynamics. During one period of the orbit these phaseshifts multiply up to the $\chi_m(g_p)$ in (17). Two-dimensional representations are more complicated.

The phase index ($a > 0$) is found to equal the length of the symbol sequence, i.e. $\mu_p = n_2 + n_1 + n_0$. This corresponds to a phase loss $\pi/2$ for every reflection of the

potential (not counting the reflection of the domain walls), and is confirmed by explicit calculation according to [2] and [22] for a large number of orbits.

The phase indices in the hyperbola billiard ($a = 0$) are obtained using the fact that each bounce on a hard wall acquires a phaseshift π in the wavefunction, i.e. $\mu_p = 2(n_2 + n_1 + n_0)$.

The phase indices and the signs of the eigenvalues might change in connection with a pruning cascade (see figure 4)!

Due to the homogeneity of the Hamiltonian it suffices to study the classical motion at a single fixed energy; we choose $E_0 = \frac{1}{2}$. We introduce a scaled energy $k(E)$ and express the action integral $S_{\tilde{p}}$ as $S_{\tilde{p}} = T_{\tilde{p}}(E = E_0)k(E)$; $k(E)$ is found from the scaling relations and the familiar identity $T_p = \partial S_p / \partial E$:

$$k(E) = \frac{2}{a+2}(2E)^{(a+2)/4}. \tag{18}$$

The other orbit invariants are dimensionless and hence independent of energy.

With the M least unstable periodic orbits one can construct the $N \approx 1.3M$ first pseudo-orbits (see [21]). Due to the intermittent behaviour of the system, great care has to be taken so that one really gets the M least unstable orbits; the stability exponent is not simply proportional to the length of the symbol string like in a typical hyperbolic system (which is the case in [10]). This may be illustrated by the following example: among the $M = 135$ least unstable orbits in the hyperbola billiard the one with the longest symbol string has length 40, but there are about 10^{17} orbits with length 40! When $a > 0$ complications arise due to sequences like $.220^k.$, for which the stability index is not a monotonous function of k. This phenomenon is connected with the pruning for a certain $k > k_{\max}$.

After these precautions we feel confident that we have obtained the 135 least unstable orbits in the hyperbola billiard and the 70 in the x^2y^2 potential. In the x^2y^2 potential we have excluded all orbits contributing to the bifurcation cascade in figure 3. Due to the smallness of the corresponding KAM island it cannot support any quantum states unless they have very high energy. This is achieved through a subtle interference of the (infinitely many) stable and unstable orbits in the stability island. Since it is certainly not straightforward to include stable orbits in (16) we exlude these stable orbits together with the unstable ones. The exclusion of these orbit from the calculation might induce a small shift in energies even for the lower states studied in this article. Only the first 12 orbits in the x^2y^2 potential in the sequences $.20^k.$ and $.110^k.$, respectively, have been calculated explicitly. The invariants for the rest of these sequences are obtained from the fact that, asymptotically, Λ and S^2 increase linearly with k to a high degree of accuracy, as can be shown using the adiabatic approximation.

We search for zeros of $Z_N(E)$ in the complex k-plane rather than in the E-plane. The results (see tables 1 and 2 and figure 5) strongly indicate that it is possible to calculate individual eigenstates with a finite number of pseudo-orbits. With the number of orbits used in figure 5 the first six (eight) eigenvalues of the x^2y^2 potential (hyperbola billiard) are resolved. If more orbits are added more levels will eventually be resolved. What typically happens is that (i) the resolved zeros converge to their final positions and (ii) at higher $k(E)$ new zeros are created, or old zeros split, start to approach the real k-axis, eventually to be associated with the quantum states.

One clearly sees from figures 6 and 8 that the zeros converge to positions in a neighbourhood of the real k-axis and that the real parts are close to the exact quantum mechanical values. (Some pseudo-orbits are lacking for $100 < n < 200$ in the x^2y^2 case.)

Table 1. Zeros of $Z_{N=104}(k)$ in the strip $0<\mathrm{Re}(k)<3.5$, $-0.5<\mathrm{Im}(k)<0.5$ for the x^2y^2 potential in the A_1 representation. Zeros close to the real k-axis are associated with quantum eigenvalues (third column).

Re(k)	Im(k)	k_{QM}
0.1386	−0.1221	
0.6562	−0.1212	
0.7005	0.0687	0.7201
1.3809	−0.1677	
1.7495	−0.3186	
1.7778	−0.0628	1.7114
2.1993	0.0042	2.2241
2.6327	−0.0005	2.6312
3.0025	−0.0144	2.9856
3.3090	−0.0731	3.3037

Table 2. Zeros of $Z_{N=141}(k)$ in the strip $4<\mathrm{Re}(k)<10$, $-0.3<\mathrm{Im}(k)<0.3$ for the hyperbola billiard in the A_2 representation. Zeros close to the real k-axis are associated with quantum eigenvalues (third column).

Re(k)	Im(k)	k_{QM}
4.0990	−0.1512	
4.5269	−0.1382	
4.6254	−0.0497	4.632
4.7906	−0.2307	
5.1406	−0.1704	
5.4507	−0.2049	
5.8551	−0.1619	
6.0586	−0.0082	6.023
7.0018	−0.0044	7.031
7.0649	−0.1946	
7.7891	−0.0390	7.714
8.1153	−0.1073	8.243
8.6820	−0.0877	8.777
8.8107	−0.2335	
9.1612	−0.1113	9.287
9.8429	−0.0772	9.863

The quantum mechanical data are cited from [9] for the hyperbola billiard and [23] for the x^2y^2 potential.

There are additional (spurious) zeros, especially among the lower states. However, these tend to keep away from the real k-axis as $N\to\infty$. The behaviour of a typical spurious zero is seen in figure 7. Generally, one expects generations of non-leading zeros of the Selberg product (see [24]). This phenomenon is probably an artifact induced by the stationary phase approximation leading to (1).

We note (see figure 8) that the convergence in the x^2y^2 system is more convincing than in the hyperbola billiard. This fact may be attributed to finite sequences of the form $p_0 0^k$. They are generally pruned for much higher k_{max} in the hyperbola billiard than in the x^2y^2 model. Since Λ increases more slowly than linearly for these finite sequences they will cause convergence problems for the hyperbola billiard while the x^2y^2 model will be more dominated by the infinite sequences $.20^k.$ and $.110^k.$.

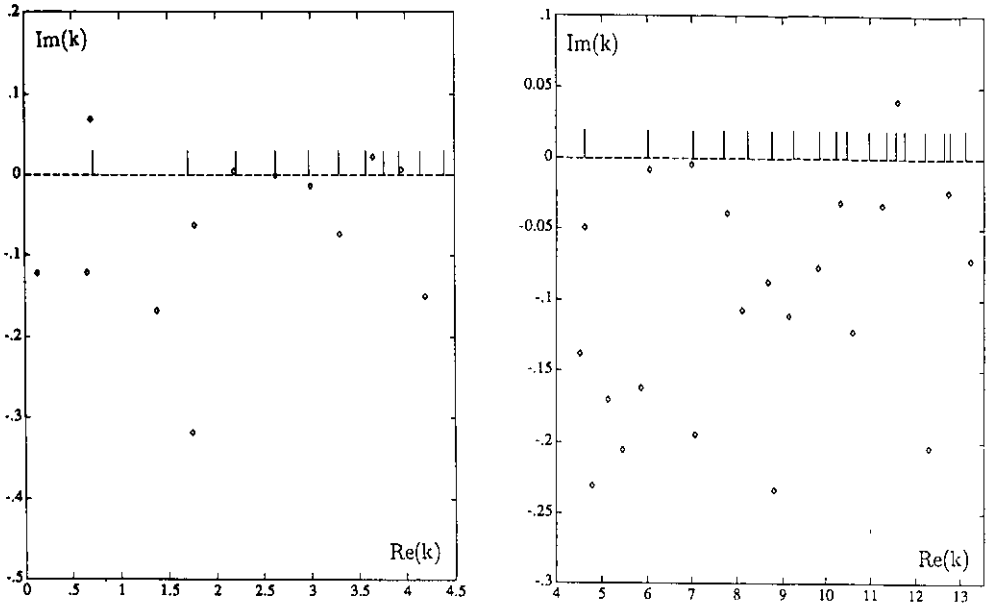

Figure 5. (*a*) Zeros of $Z_{N=104}$ in the complex k-plane (x^2y^2 potential in representation A_1). (*b*) Zeros of $Z_{N=141}$ in the complex k-plane (hyperbola billiard in representation A_2). Quantum mechanical values are indicated by vertical bars on the real axis.

5. Discussion

The fact that the phase index μ_p in the hyperbola billiard turns out to be twice as large as the corresponding index in the quartic potential may seem like a very disturbing discontinuity in the limit $a \to 0$. In this connection it is instructive to compare semiclassical (WKB) and quantum mechanical energy levels in the one-parameter family of potentials $V = (x^2)^{1/a}$. For the harmonic oscillator ($a = 1$) the WKB calculation happens to yield the exact quantum mechanical result (with a phase index of 2). When decreasing a, however, the WKB results get increasingly worse, especially for low-lying states. In the limit $a \to 0$ (infinite square well) the semiclassical results suddenly turns exact again, provided one *doubles* the phase index. One could in principle obtain better semiclassical results by letting the phase index interpolate between 2 and 4, and it would certainly be nice to derive such an interpolating relation, though this is far outside the subject of this paper.

We note that there is a close connection between the expansion (16) and the curvature expansions in [10, 25]. In the latter the zeta function is written as $Z(E) = \Pi_p(1 - t_p) = 1 - \Sigma_f t_f - \Sigma_n c_n$, where $\Sigma_f t_f$ is a sum over the *fundamental* orbits, i.e. orbits that cannot be approximated in terms of shorter ones, and $\Sigma_n c_n$ is the *curvature* contribution to the sum. The curvature corrections c_n are built from longer orbits (not fundamental) minus their approximations in terms of shorter, shadowing orbits. In a truly hyperbolic system, e.g. the open three-disc system studied in [10]), the corrections fall off faster than exponentially. If on the other hand the symbolic dynamics is pruned the alphabet has to be redefined, in order to have a well-converging curvature expansion. This leads in general to an infinite number of fundamental orbits. If the *grammar* is *finite*, i.e. there is a finite set of pruning rules, there exist schemes for a systematic

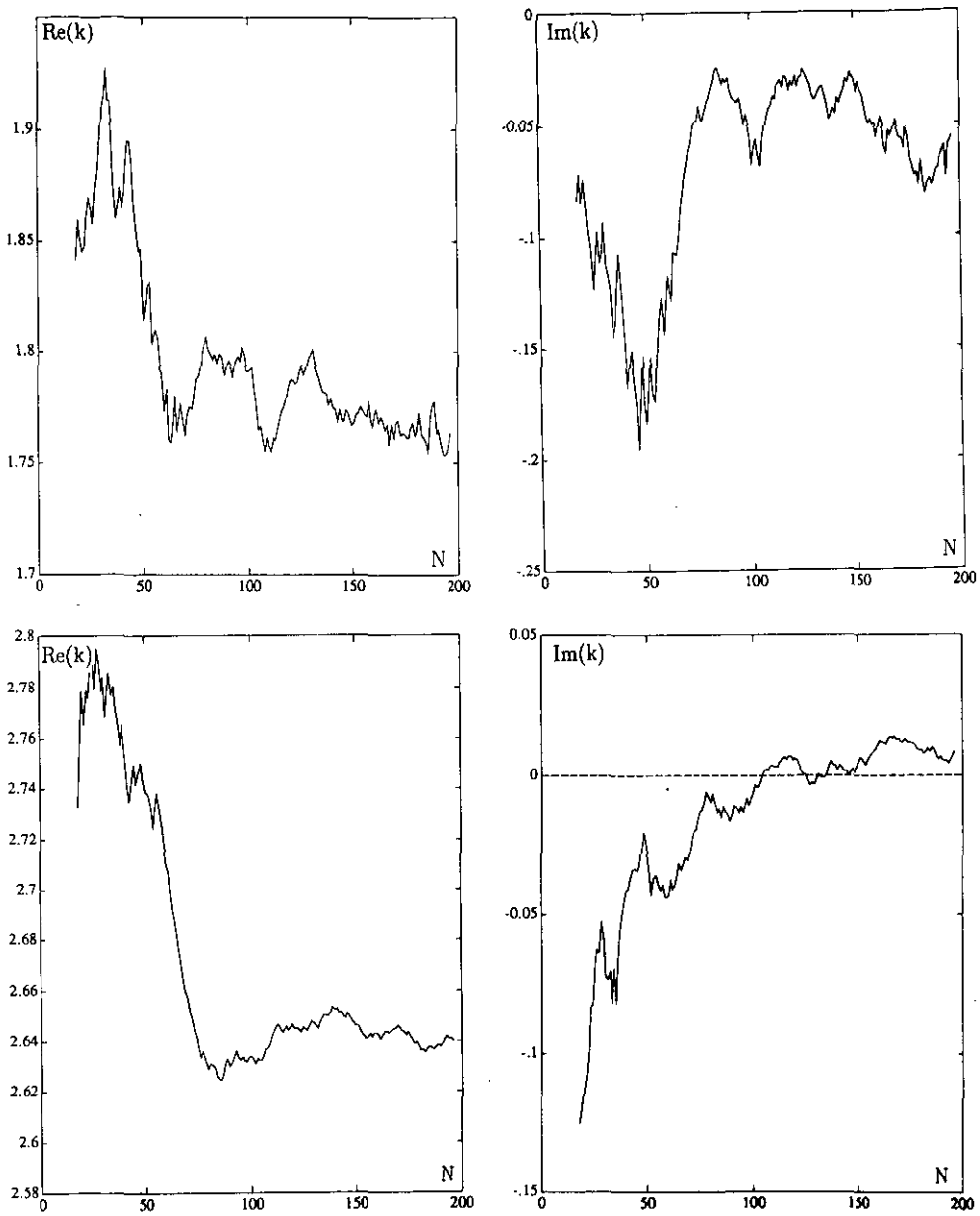

Figure 6. Convergence of the real and imaginary part of the zeros k of $Z_N(k)$ associated with the (a) second and (b) fourth eigenstates (x^2y^2 potential in the A_1 representation).

construction of this redefined symbolic dynamics [26, 27]. However, even in very simple found systems, e.g. a closed three-disc system, a finite grammer has not yet been found. The problem of finding a curvature expansion for a specific system easily gets infinitely complicated.

The expansion (16) has the advantage of being independent of the symbolic dynamics. If we apply it to the open three-disc scattering system we would regain the curvature expansion of [10], (provided one cuts off the expansion for appropriate N).

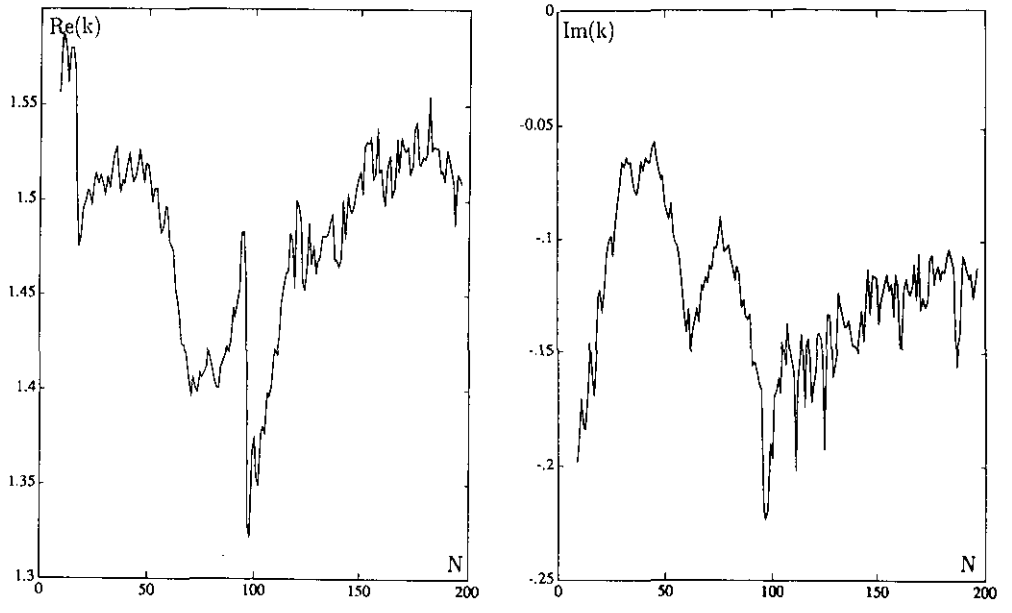

Figure 7. Typical behaviour of a zero of Z_N not associated with any quantum state (x^2y^2 potential in the A_1 representation).

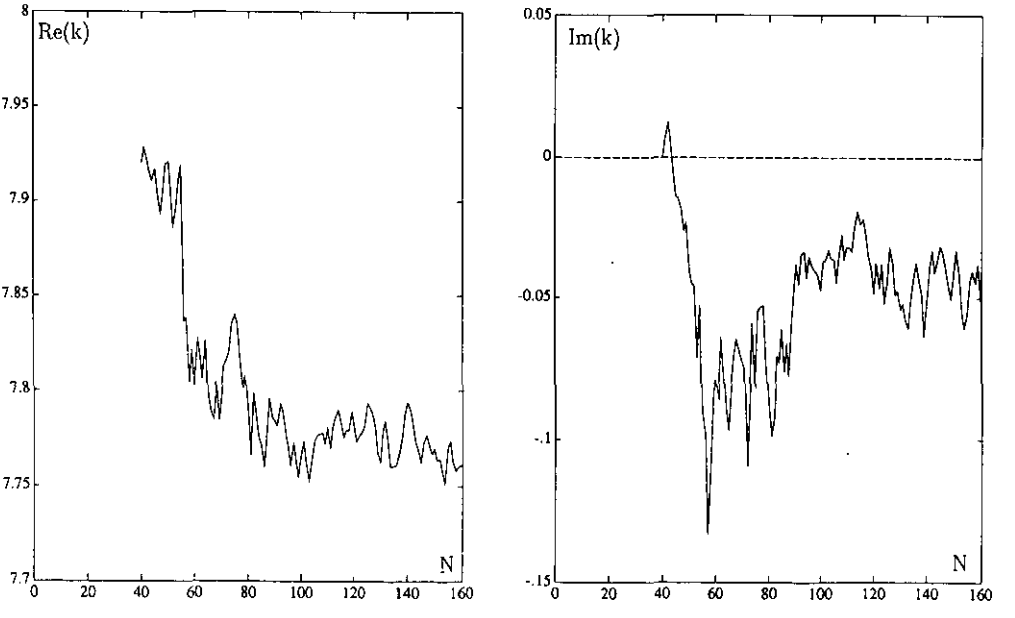

Figure 8. Convergence of the real and imaginary parts of the zeros of $Z_N(k)$ associated with the fourth eigenstates (hyperbola billiard in the A_2 representation).

The expansion will adjust itself for complications (i.e. deviations from hyperbolicity) that arise naturally in bound systems, e.g. intermittency, long orbits with anomalously low instability and pruning of the symbolic dynamics.

If one does not have a good grammar for the system, the expansion (16) is a very natural object to use. However, if one could find a proper shadowing scheme, prerequisiting a good control of the symbolic dynamics and its pruning rules, the result would probably be improved. This means that one could be able to group the pseudo-orbits in such a way that a shadowed orbit is placed on the same side of the cut-off N as the shadowing pseudo orbit. This would naturally decrease the oscillations that are now superposed on the convergence. We hope to return to these questions in future work.

There has been much interest focused on the formal similarity between the Selberg zeta function for a chaotic system and the Riemann zeta function [21, 28]. The non-trivial zeros of the Riemann zeta function are (according to Riemann's hypothesis) centred on the strip where the Euler product and the Dirichlet series representations of it diverges. It would be tempting to generalize this fact and claim that the Selberg zeta function for a generic chaotic system is divergent, but such a generalization is dangerous since the Selberg zeta function has a totally different analytic structure due to the product over k (see (3)). The occurrence of phase indices in a dynamical system (they are absent in the Riemann case) might also have importance for the convergence. *If* the trace formula is convergent (for some systems at least) it is *conditionally* convergent and there is therefore a potential danger of obtaining different results from different summation techniques.

In a paper by Berry and Keating [21] a resummation technique based on an analogy with a derivation of the Riemann–Siegel formula is presented, based on a self-duality of the Riemann zeta function. However, as the authors themselves note, such a self-duality for a general chaotic system would require a 'miraculous conspiracy' which we have no reason to expect to hold exactly, although this and related ideas to use the knowledge of the mean level density in a resummation scheme might very well be fruitful [29-31].

Acknowledgments

We would like to thank P Cvitanović, B Eckhardt, D Wintgen and F Christiansen for interesting discussions and S E Rugh for pointing out some relevant references to us.

References

[1] Gutzwiller M C 1990 *Chaos in Classical and Quantum Mechanics* (New York: Springer)
[2] Gutzwiller M C 1967 *J. Math. Phys.* **8** 197; 1969 *J. Math. Phys.* **10** 1004; 1970 *J. Math. Phys.* **11** 1791
[3] Miller W 1975 *J. Chem. Phys.* **63** 996
[4] Voros A 1988 *J. Phys. A: Math. Gen.* **21** 685
[5] Balazs N and Voros A 1986 *Phys. Rep.* **143** 109
[6] Gutzwiller M C 1980 *Phys. Rev. Lett.* **45** 150; 1985 *Phys. Scr.* T **9** 184; 1986 *Cont. Math.* **53** 215
[7] Aurich R and Steiner F 1989 *Physica* **39D** 169
[8] Gutzwiller M C 1982 *Physica* **5D** 183; 1988 *J. Phys. Chem.* **92** 3154
[9] Sieber M, and Steiner F 1990 *Physica* **44D** 248; 1990 *Phys. Lett.* **148A** 415

[10] Cvitanović P and Eckhardt B 1989 *Phys. Rev. Lett.* **63** 823
[11] Russberg G 1991 in preparation
[12] Eckhardt B and Wintgen D 1990 *J. Phys. B: At. Mol. Opt. Phys.* **23** 355
[13] Christiansen F 1989 Analysis of chaotic dynamical systems in terms of cycles *Master thesis* Niels Bohr Institute, University of Copenhagen
[14] MacKay R S and Meiss J D 1987 *Hamiltonian Dynamical Systems* (Bristol: Adam Hilger)
[15] Matanyan S G, Savvidy G K and Ter-Arutyunyan-Savvidy N G 1981 *Sov. Phys.-JETP* **53** 421
[16] Dahlqvist P and Russberg G 1990 *Phys. Rev. Lett.* **65** 2837
[17] Roukes M L, Scherer A and Van der Gang B P 1990 *Phys. Rev. Lett.* **64** 1154
[18] Robbins J 1989 *Phys. Rev.* A **40** 2128
[19] Lauritzen B 1991 *Phys. Rev.* A **43** 603
[20] Cvitanović P and Eckhardt B 1991 *Nonlinearity* submitted
[21] Berry M V and Keating J P *J. Phys. A: Math. Gen.* **23** 4839
[22] Creagh S, Robbins J and Littlejohn R 1990 *Phys. Rev.* A **42** 1907
[23] Martens, C C, Waterland R L and Reinhardt W P 1989 *J. Chem. Phys.* **90** 2328
[24] Cvitanović P 1991 *Applications of Chaos, Electrical Power Research Institute Workshop 1990* ed J H Kim and J Stringer (New York: Wiley)
[25] Artuso R, Aurell E and Cvitanović P 1990 *Nonlinearity* **3** 325, 361
[26] Cvitanović P 1991 *Proceedings of the Los Alamos Center for Nonlinear Science, Nonlinear Science—Next Decade, May 1990* (to appear in *Physica* **D**)
[27] Grassberger P 1988 *Z. Naturforsch.* **43a** 671
[28] Berry M V *Quantum Chaos and Statistical Nuclear Physics. Springer Lecture Notes in Physics* vol. 263 ed T H Seligman and H Nishioka (Berlin: Springer) pp 1–17
[29] Bogomolny E B 1991 Semiclassical quantization of multidimensional systems *Preprint* Orsay IPNO/TH91
[30] Tanner G *et al* 1991 Quantum eigenvalues from classical periodic orbits *Preprint* Freiburg, Marburg, Heidelberg, March 1991
[31] Sieber M and Steiner F DESY 1991 On the quantization of chaos *Preprint* 91-017